The Role of Silanols in the Interactions between Methyl tert-Butyl Ether and High-Silica Faujasite Y: An Infrared Spectroscopy and Computational Model Study

UNIVERSITÀ DEGLI STUDI DI TORINO

Interactions between methyl *tertiary* butyl ether and high silica faujasite Y elucidated by infrared spectroscopy: an experimental and computational model study of involved silanols

Ilaria Braschi [a,b*], Giorgio Gatti[b], Chiara Bisio[b,c], Gloria Berlier[d], Vittoria Sacchetto[b], Maurizio Cossi[b], Leonardo Marchese[b*]

[a] *Dipartimento di Scienze e Tecnologie Agroambientali, Università di Bologna, V.le G. Fanin 44 - 40127 Bologna (Italy)*

[b] *Dipartimento di Scienze e Tecnologie Avanzate and Centro Nano-SiSTeMI, Università del Piemonte Orientale "A. Avogadro",Via T. Michel 11 - 15121 Alessandria (Italy)*

[c] *ISTM-CNR Istituto di Scienze e Tecnologie Molecolari, via G. Venezian 21, Milano (Italy)*

[d] *Dipartimento di Chimica IFM and NIS Centre of Excellence, Università di Torino, Via P. Giuria 7 - 10125 Torino (Italy)*

* *Correponding authors e-mail:* ilaria.braschi@unibo.it; leonardo.marchese@mfn.unipmn.it

ABSTRACT

It is generally believed that the retention of methyl *tertiary* butyl ether (MTBE) by zeolites is positively correlated to the silica content of these materials. Nevertheless highly dealuminated zeolites can contain relevant amount of silanol groups. In this study the effect of these point defects in a zeolite Y (SiO_2/Al_2O_3 = 200) on the adsorption of MTBE was evaluated by means of infrared spectroscopy, supported by DFT calculations. The adsorption process is found to occur in two steps, involving isolated silanol sites and the siloxane network of the zeolite, respectively, with an average loading of 1.3 molecules per cage in the first and 1.3 molecules in the second stage. Both external and internal isolated silanol groups (stretching at 3746 and 3738 cm^{-1}, respectively) are involved in the MTBE adsorption process with the formation of H-bonded complexes and associated shifts (516 cm^{-1} and 358 cm^{-1}, respectively) consistent with a H-bonding strength higher for external than for the internal ones. However, MTBE is more tightly adsorbed on the internal silanols as a result of the cage confinement effect. The band assigned to the methyl symmetric stretching of CH_3O- group can be used to discriminate between H-bond and van der Waals MTBE-zeolite interactions (2843 and 2828 cm^{-1}, respectively). *Ab initio* models were used to compute the harmonic frequencies of different MTBE-zeolite models and to simulate the cage confinement of one and three ether molecules.

Keywords: High silica zeolite, MTBE, adsorption, microgravimetry, FTIR, *ab initio* calculations.

Introduction

Fuel-based pollutants are commonly present in soil and ground water coming from areas where refinery plants and gas stations are located. To restrict downward movement of contaminants along the soil profile and to clean-up polluted deep waters, permeable reactive barriers, made of a continuous synthetic layer of sorbent materials, can be used [1,2]. The information needed to properly scale these barriers includes the nature and strength of interactions between pollutants and barrier fillers.

Methyl *tertiary* butyl ether (MTBE) has been used as a fuel additive since 1979 to increase the oxygenate content of the gasoline which reduces harmful tailpipe emissions [1]. Although it is used as an agent to control air pollution, inevitable releases of MTBE into the environment cause contamination of drinking water resources and there is evidence that it is a possible human carcinogen [2]. An additional problem caused by its high aqueous solubility (ca. 50 g L^{-1} at room temperature) and low vapour pressure (100 mbar at 20°C) consists in the difficult removal of this contaminant from water with treatment processes such as air stripping or adsorption on activated carbon [1,3]. As an alternative to these techniques, high silica zeolites (i.e. mordenite, silicalite, faujasite, and others) have been investigated as possible sorbents of MTBE from water [4-8]. Contrarily to what happens with activated carbon, the adsorption of MTBE into zeolites is not affected by the natural organic matter always present in natural waters [9]. In addition, the useful life of zeolitic materials is ca. 5-6 times longer than that of activated carbon [9].

It is generally assumed that the MTBE adsorption process is driven by the zeolite hydrofobicity (expressed by the SiO_2/Al_2O_3 ratio) [10,11]. However, dealuminated zeolites are known to be defective and to contain silanol groups whose role in this process is not yet clarified.

In this study, the contribution of different silanol groups in a defective high silica zeolite Y to the adsorption of MTBE has been studied by infrared spectroscopy, supporting the experimental data with computational models and *ab initio* calculations. Since it is known that this kind of zeolites contains both isolated and H-bonded silanols [12,13], we considered the vibrational pattern of different groups, illustrated in Figure 1. Since it is knowledge of the authors that MTBE displaces water molecules previously H-bonded to zeolite silanols (data unpublished) owing to its higher Lewis base character, the present study has

been performed on dehydrated zeolite. The key factors driving the adsorption process have been enlightened.

Experimental methods

A. Materials. Methyl *tertiary* butyl ether (MTBE) was purchased as analytical standards by Sigma-Aldrich with a purity of 99.9%. Highly dealuminated (high silica) zeolite Y (herafter named HSZ-Y) powder in protonated form with 200 SiO_2/Al_2O_3 molar ratio (code HSZ-390HUA) and a standard zeolite Y (hereafter named SZ-Y) powder in protonated form with 5.1 SiO_2/Al_2O_3 molar ratio (code CBV 400) were purchased from Tosoh Corporation (Japan) and from Zeolyst (USA), respectively.

The specific surface area (SSA) of both zeolites was measured by means of nitrogen adsorption at liquid nitrogen temperature (-196°C) in the pressure range $7 \cdot 10^{-6}$ to 1013 mbar (1 mbar = 100 Pa) using an Autosorb-1-MP (Quantachrome Instruments). Prior to adsorption, the samples were outgassed for 1 h at 90°C, 1 h at 130°C, and finally 16 h at 300°C under high vacuum conditions (final pressure $1 \cdot 10^{-9}$ mbar). The specific area of HSZ-Y and SZ-Y was determined by the Brunauer−Emmett−Teller (BET) approach and using 0.01 as the value of maximum relative pressure. The pore size distribution was calculated by applying the cylindrical pore NLDFT method in the desorption branch.

B. Adsorption isotherms. MTBE adsorption isotherms were obtained at 35°C on the HSZ-Y sample outgassed for 4 h at 35 and 400°C employing an intelligent gravimetric analyzer (IGA-002, Hiden Analytical Ltd., UK), with integrated temperature and pressure controllers. The former consists in a thermostated water bath/circulator, employing a 50% water : 50% antifreeze (inhibited ethylene glycol) mixture. The latter is based on two pressure sensors, working in the 0-10 mbar (Baratron capacitance manometer, accuracy ± 0.05 mbar) and 10-1000 mbar (strain gauge, accuracy ± 1 mbar) ranges. IGA is an ultrahigh-vacuum (UHV) microbalance (weighing resolution 0.2 μg), specifically designed to study vapour sorption, which allows isotherms and the corresponding kinetics of adsorption and desorption to be determined, for set pressure steps. Buoyancy corrections were carried out using the weights and densities of all the components of the sample and counterweight sides of the balance and the measured temperature.

The mass uptake was measured as a function of time, and the approach to equilibrium of the mass relaxation curve was monitored in real time using a computer algorithm (real time processor RTP).

For each isotherm point, the time origin (t0) of real-time analysis was set at 95% of the pressure change, while the minimum and maximum data collection time were set to 5 and 30 min, respectively. RTP uses last-squares regression of a linear driving force (LDF) model in order to extrapolate a value of the mass relaxation asymptote and to assess the time-scale of interaction.

LDF model of the mass relaxation u(t) (uptake at a time t) is based on the equation:

$u(t) = u0 + \Delta u(1-\exp(-[t-t'0]/k))$

where u0 is the uptake at arbitrary time origin t'0, k is the exponential time constant and Δu is the change in uptake. The asymptotic value is then equal to u0 + Δu.

C. FTIR Spectroscopy. Infrared spectra were collected on a Thermo Electron Corporation FT Nicolet 5700 Spectrometer with 1 cm^{-1} resolution. Self-supporting pellets of HSZ-Y samples were obtained with a mechanical press at ca. 7 tons cm^{-2} and placed into an IR cell equipped with KBr windows permanently attached to a vacuum line (residual pressure: ≤ $1 \cdot 10^{-4}$ mbar), allowing all treatments and MTBE adsorption/desorption experiments to be carried out *in situ*. Spectra of MTBE adsorbed on HSZ-Y have been collected at beam temperature (ca. 35°C) on samples previously dehydrated under vacuum at beam temperature or after outgassing at 700°C. Spectra of MTBE in CCl_4 solution were performed in a KBr standard cell for liquids.

Variable temperature spectra (from room temperature to 700°C) have been collected upon outgassing a HSZ-Y pellet at the desired temperature at 5°C min^{-1} heating rate. All spectra have been recorded at beam temperature.

D. Models and *Ab Initio* Calculations. All calculations have been performed with TURBOMOLE6 package [14,15] at the DFT level with B3LYP hybrid functional [16-18] and a mixed basis set, comprising 6-31G(d,p) [19,20] atomic basis (a widely used Pople's double-z set plus polarization functions) on oxygen and hydrogen atoms, and Hay and Wadt [21] effective core potentials (ECP) and basis set on silicon. After geometry optimization, the harmonic frequencies were computed at the same level.

Different models were used to study the adsorption of MTBE on the silica framework: first, a small cluster ($Si_{13}O_{13}H_{28}$) was defined to reproduce a portion of the surface, with an isolated Si-OH group (see Figure 2a): all the silicon free valences were saturated with fictitious H atoms. This structure was also modified substituting one of the terminal hydrogen atoms with a second OH group, H-bonded to the central silanol (Figure 2b). Such models were used to study the interactions between the ether molecule and isolated or H-bond acceptor silanols, also computing the harmonic vibrational spectra.

A larger model was used to describe the zeolite cage, as described in ref. [22]. The HSZ-Y unit cell comprises eight cages of approximately tetrahedral shape: a single cavity was extracted from the crystallographic structure [23] and all the free valences on Si atoms were saturated with outward pointing OH groups, so that the cage model was comprised by 48 Si atoms, 72 O atoms in the cage walls, and 48 OH groups. In this "ideal" cage, no real silicon groups are present (since the external OH groups are computational artifacts, only used to remove the Si dangling bonds): then a defect was introduced in the model, removing one Si atom from the wall and generating three additional Si-OH groups. The geometry of the silanol groups was adjusted to leave just one Si-OH available for binding the guest molecule inside the cage, in order to model an isolated silanol (*vide infra*). The cage model is shown in Figure 3a.

Results and Discussion

The faujasite Y, selected for this adsorption study on the basis of its pore dimension, high hydrophobicity and defectivity, was a high silica zeolite (HSZ-Y). The defectivity of HSZ-Y was previously attested by the composition of the unit cell that was defined as $Si_{186}O_{360}(OH)_{24}$ [22], giving, as a result, three silanol groups per cage on average (being the unit cell formed by eight cages). In the calculation the content of aluminum was assumed negligible, being 1 atom per 400 silicon atoms.

Material Characterization

The structure of faujasite Y is characterized by approximatively 12 Å diameter cages, which are linked through access windows of 7.0 Å × 7.1 Å in diameter and are composed of rings of twelve linked tetrahedra (12-membered rings) [24]. These cages and windows permit quite large molecules to enter [22,23], making

this structure potentially useful in the adsorption of MTBE. The selected HSZ-Y structure has been investigated by means of pore size distribution analysis and variable temperature FTIR spectroscopy.

Textural properties. Measurements of pore size distribution were performed on both standard (SZ-Y) and dealuminated (HSZ-Y) zeolite in order to verify at which extent the dealumination process modified the pore architecture of the starting zeolite.

Figure 4 shows that the pore size distribution of SZ-Y is centred at ca. 11 Å, a dimension typical of zeolite Y α cage diameter. For the same material, mesopore diameters from 30 to 100 Å, due to particle aggregation, were also found. In the HSZ-Y sample, the structural pore diameter distribution is spread between 10 and 40 Å with two main pore sizes at ca. 13 and 22 Å. A specific surface area (SSA) of 902 m^2 g^{-1}, half of which due to the presence of micropores (437 m^2 g^{-1}) with related volume of 0.32 m^2 g^{-1}, was determined (Table 1). As expected, because of the dealumination process, both the micropore SSA and volume were lower if compared with those of the standard zeolite (SSA = 543 m^2 g^{-1} and V_{microp} = 0.47 cm^3 g^{-1}, respectively). Beside micropores of 13 Å, intraparticle mesopores of dimension between 20 and 40 Å and volume of 0.16 cm^3 g^{-1} were found for the HSZ-Y sample. It was therefore inferred that the dealumination process noticeably affected the HSZ-Y pore architecture, enlarging the windows between interconnected cages and thus forming mesopores [25]. This process led also to the production of a significant concentration of internal silanols [26], which affect the MTBE adsorption (*vide infra*).

Variable temperature infrared spectra of high silica zeolite Y. Figure 5A shows the IR spectra recorded at increasing outgassing temperature, along with that of the sample exposed to air (curve a). The latter spectrum presents a narrow band at 3746 cm^{-1} (expanded view in Fig. 5B), due to the OH stretching mode of isolated silanol groups (Fig. 1, structure (1)) essentially located on the external surface of the zeolite particles [12], and a very broad band extending in the region between 3700 and 2900 cm^{-1} due to the stretching modes of both H-bond donor silanol (Fig. 1, structure (2)) and water hydroxylic groups [13]. The presence of water adsorbed on the zeolite (ca. 1 w%, [22]) is also confirmed by the bending mode at 1633 cm^{-1} (Fig. 5A, inset).

Upon outgassing the zeolite pellet at room temperature (curve b), the contributions of the adsorbed water disappear and, in parallel, a band at ca. 3738 cm^{-1}, strongly overlapped to the band at 3746 cm^{-1}, is formed. Bands in similar position have been very often observed in defective zeolites [12] and in porous silicas [27] and are assigned to isolated silanol groups located inside microcavities. This is a clear indication that water molecules are mostly bound to internal silanols. The broad band still present after water removal in the range 3700-3200 cm^{-1} with a maximum at ca. 3530 ± 5 cm^{-1}, is due to H-bond donor silanols (Fig. 1, structure (2)) [12,13]. The H-bond acceptor silanols (Fig. 1, structure (3)), are expected in the range 3735-3725 cm^{-1} [12,13] and they are not clearly distinguishable from the internal isolated silanols at 3738 cm^{-1}.

The outgassing of HSZ-Y up to 700°C (curves c-g) gradually reduces the intensity of the broad band of H-bonded silanol groups and isolated species are contemporarily formed, as testified by the increasing of the bands at 3746 and 3738 cm^{-1}. The former band becomes more and more dominant at the highest outgassing temperatures.

To support the above interpretation of the silanol spectra, the harmonic frequencies were computed at the DFT level for two models of isolated and H-bonded silanols, respectively (Figure 2, structures a and b). The computed stretching frequencies were 3806, 3788 and 3590 cm^{-1} for isolated, H-bond acceptor and H-bond donor silanols, respectively. Though the harmonic frequencies are systematically overestimated, as expected, their differences are closer to the experimental counterparts. For instance the computed stretching frequencies for isolated and H-bond donor silanols differ by 216 cm^{-1}, in very good agreement with the experimental difference of 211-221 cm^{-1}.

MTBE adsorption in high silica zeolite Y

The contribution of different type of HSZ-Y silanols to the MTBE adsorption was evaluated by microgravimetry and FTIR measurements on both dehydrated and outgassed zeolite samples at increasing temperature.

Adsorption isotherms. The gravimetric MTBE isotherms measured at 35°C on the sample pretreated in vacuo at the same temperature are reported in Figure 6. Three different regimes can be determined by the

analysis of the curves, both in adsorption and in desorption branches. The first derivative of the curves (data not shown) clearly indicates that there is a slope change at 1.25 mbar. At pressures lower than 1.25 mbar, the MTBE uptake as a function of equilibrium pressure is very steep, then the curve slope decreases up to 10 mbar, when it gradually comes to a plateau. These trends testify the different strength of interactions between MTBE and HSZ-Y adsorbent in the three regimes. Between 0 and 1.25 mbar, MTBE uptake determined using the desorption branch is of 8.1% zeolite dry weight (DW) corresponding to 1.3 molecule per cage; between 1.25 and 10 mbar, the uptake is of 7.0% zeolite DW corresponding to 1.1 additional molecule per cage; and from this pressure upwards, MTBE overall uptake equals to 16.4% zeolite DW accounting in total for 2.6 molecules per cage.

In agreement with IR results (*vide infra*), at low pressures MTBE molecules interact with silanol groups forming 1:1 silanol/MTBE H-bonded complexes, at pressure higher than 1.25 mbar the adsorption is likely driven by van der Waals interactions between zeolite walls and MTBE molecules (host-guest) and between MTBE molecules (guest-guest), which further cause condensation at pressure higher than 10 mbar.

The objective of the real-time analysis performed during the measurements is to ensure that the sorption-time curve is determined with sufficient time resolution and for sufficiently long to enable such analyses. Thus, we will not enter here in the details of the isotherm kinetics.

The isotherms of MTBE adsorbed on the sample pretreated at 400°C showed very similar results of the overall mass uptake (ca. 16% zeolite DW, data not shown) with respect to the sample pretreated at 35°C. Notably, also in the low pressure regime (0-1.25 mbar) the uptake is very similar being ca. 8% zeolite DW at 1.2 mbar. This result means that: i) the number of silanol groups interacting with MTBE is similar after sample treatment at both 35 and 400°C; ii) the H-bonded silanols present in the zeolite dehydrated at 35°C are not significantly involved in the MTBE adsorption.

Experimental and computational MTBE IR spectra. The interpretation of IR spectra of MTBE adsorbed on HSZ-Y from the gas phase (see next section) was facilitated by comparing the observed bands with theoretical harmonic frequencies computed in vacuum (Fig. 7,a) and those of the experimental spectra of the molecule both in gas phase (curve b) and dissolved in carbon tetrachloride (curve c). The latter

spectrum is particularly useful in that, when the pollutant was adsorbed into the zeolite cavities, the IR pattern was expected to resemble that of the molecule diluted in a non polar solvent because of the non polar nature of the high silica zeolite cage. The computed harmonic frequencies are systematically overestimated, but the spectrum pattern is reproduced accurately enough to allow the interpretation. The main features of the whole experimental spectra are well reproduced by the calculations (Table 2) and are in good agreement with the work of Li and Singh [28].

For the purpose of this paper, the main IR features will be described in the following. The MTBE spectrum in the gas phase (curve b) shows a more complex pattern than in carbon tetrachloride solution (curve c) because some vibrational modes clearly display the rotational contribution.

In the high wavenumber region (3000-2800 cm^{-1}), the spectrum in CCl_4 solution shows two well defined bands at 2974 and 2939 cm^{-1} that are assigned to CH_3 asymmetric stretching of *tertiary* butyl and methoxyl radicals, respectively, and at 2827 cm^{-1} due to CH_3 symmetric stretching of the methoxyl group (please, notice that an arbitrary definition of methoxyl radical is used in this paper in order to distinguish the methyl group directly bound to the etheric oxygen from those of *tertiary* butyl radical). These absorptions can be used to distinguish different MTBE phases (i.e. the molecule in the adsorbed or in the gas phase). In the region 2920-2850 cm^{-1}, a complex absorption due to CH_3 symmetric stretching mode of *tertiary* butyl radical is found.

At low wavenumber of MTBE in CCl_4, two well resolved bands at 1386 and 1364 cm^{-1} are assigned to symmetric deformations (i.e. umbrella mode) of CH_3 groups of *tertiary* butyl radical with different vibration phase (i.e. in the 1386 cm^{-1} mode all three methyl groups open and close contemporarily, whereas in the 1364 cm^{-1} mode two methyl groups close and one opens). These bands could be used as markers for the molecule in a solvated state as experienced when adsorbed into the zeolite cage.

Unfortunately the spectral region extending below 1300 cm^{-1} cannot be used for predicting interaction type and strength upon MTBE adsorption because it is masked by the strong absorptions of the zeolite lattice.

IR spectra of MTBE adsorbed on HSZ-Y. In order to highlight the types of interactions occurring between MTBE and zeolite adsorption sites as defined by the three branches of the adsorption isotherm (0-

1.25, 1.25-10 and 10-30 mbar of MTBE pressure), HSZ-Y was exposed to MTBE doses of 1.25, 10 and 30 mbar. Figure 8 shows only the infrared spectra of HSZ-Y exposed to 1.25 and 30 mbar of MTBE because there are not significant differences in the spectra recorded at 10 and 30 mbar MTBE pressure. The spectrum of the bare zeolite outgassed at room temperature is reported for comparison (curve a).

When HSZ-Y is exposed to 1.25 mbar of MBTE (curve b), the bands of isolated silanol groups at 3746 and 3738 cm^{-1} almost completely disappeared and, contemporarily, two strongly overlapped broad bands at ca. 3380 and 3240 cm^{-1} are formed. This downshift is consistent with the formation of silanol groups H-bonded to MTBE oxygen atom; a similar shift of ca. 500 cm^{-1} was in fact found by interaction of diethylether with isolated silanol groups of mesoporous silica SBA-16 [29].

The harmonic frequencies were computed at the DFT level for two models of the MTBE-silanol complex (Figure 2, structures c and d), where the ether was bonded either to isolated or to H-bond acceptor silanol groups (see the discussion above): the OH stretching frequency is 3382 cm^{-1} in the former and 3200 cm^{-1} in the latter case. Recalling the computed frequencies for the bare silanols (Figure 2 a, b), the adsorption of ether causes a frequency shift of 424 cm^{-1} for isolated and 588 cm^{-1} for H-bond acceptor silanols. The former shift is compatible with the experimental value, observed in the range 370-510 cm^{-1}, which could be thus attributed to isolated silanols (both on the external surface and inside the zeolite pores) interacting with MTBE. However, the presence of MTBE complexes with H-bond acceptor silanols cannot be excluded: combining the absorption for H-bond acceptor silanols in the bare zeolite, reported in the literature at 3735-3725 cm^{-1} [12,13], with the computed shift we would expect a band at 3147-3137 cm^{-1} for these complexes, but this signal could be masked by the intense and broad band around 3240 cm^{-1}, due to isolated silanols H-bonded to MTBE.

In the experimental spectrum at 1.25 mbar MTBE pressure (Fig. 8, curve b), MTBE H-bonded to silanol groups shows four resolved bands at 2979 and 2830 cm^{-1} and at 1390 and 1369 cm^{-1}, which are related to CH_3 stretching and bending vibrations of *tertiary* butyl group, respectively (Table 2).

At 30 mbar MTBE pressure (Fig. 8, curve c), the relative intensity of bands at 3380 and 3240 cm^{-1} changed, the latter being more pronounced than in the spectrum recorded at 1.25 mbar MTBE, and this is an evidence that adsorbate-adsorbate (i.e. guest-guest) interactions occur in the MTBE high pressure regime as shown by the computational models discussed below. In curve c, the bands related to adsorbed MTBE increased in intensity with the increase of gas dose and slightly shifted to lower frequencies at values closer to those of the spectrum of MTBE diluted in carbon tetrachloride (see Table 2). This confirms that MTBE molecules into HSZ-Y experience an environment similar to that of a non polar solvent, thus being solvated by the zeolite cage.

Nevertheless, the FTIR experiment of MTBE adsorption so far described on dehydrated HSZ-Y could not clarify if MTBE molecules interact more strongly on internal or external isolated silanols. The H-bond strength is related to the downward shift of the silanol OH stretching upon interaction with the MTBE oxygen, however, the relative position where external and internal isolated silanol groups H-bonded to MTBE oxygen absorb (i.e. at 3380 or 3240 cm^{-1}) could not be assigned. For this reason an experiment of MTBE adsorbed on HSZ-Y outgassed at 700°C (Fig. 9), where H-bonded silanols absorbing at 3700-3200 cm^{-1} are almost completely removed (Fig. 5, curve g), was performed.

The best equilibrium conditions between gas and adsorbed phase to allow all silanol groups to be bound to MTBE molecules were obtained by exposing the zeolite pellet to 2.5 mbar vapour pressure (a value slightly higher than 1.25 mbar which was gravimetrically determined) and then gradually decreasing the MTBE pressure (desorption experiment). Figure 9 shows differential IR spectra obtained by subtracting the spectrum of the bare zeolite outgassed at 700°C, and for this reason the bands related to the silanols OH stretching are negative. As said above, all silanols were consumed (most negative bands at 3746 and 3738 cm^{-1}) when the HSZ-Y sample was in contact with 2.5 mbar MTBE (Fig. 9A, curve a). In this case a broad band with maximum at 3230 cm^{-1} and a shoulder at ca. 3380 cm^{-1} was formed. This band decreased in intensity upon reduction of the MTBE dose and the component at 3380 cm^{-1} became more and more evident. In parallel, the band at 3746 cm^{-1} became less and less negative and the component at 3738 cm^{-1} progressively became more pronounced (inset of Fig. 9A). The desorption experiment clearly demonstrated

that: i) the silanol-MTBE complexes are not stable upon decreasing the MTBE pressure at beam temperature; ii) there is a correlation between the bands at 3746 (isolated external silanols) and 3230 cm^{-1} (wavenumber shift of 516 cm^{-1}), and between the bands at 3738 (isolated internal silanols) and 3380 cm^{-1} (wavenumber shift of 358 cm^{-1}); iii) upon decreasing the MTBE pressure the silanols H-bonded to MTBE absorbing at 3380 cm^{-1} are more stable than those at 3250 cm^{-1}.

It is inferred from these shifts that the MTBE molecules inside the zeolite cages form complexes with silanols via H-bonds weaker than those of MTBE bound on external silanols. However, despite the H-bond weakness, the internal silanol-MTBE complexes are more stable than the external ones because of the confinement effect inside the zeolite cages.

Methyl groups stretching and bending vibrations of the adsorbed MTBE are respectively found in the 3000-2800 and 1500-1300 cm^{-1} spectral regions (Fig. 9B). As already noticed for MTBE adsorbed in HSZ-Y degassed at room temperature (Fig. 8), all bands decrease in intensity and slightly shift to higher wavenumber upon reduction of the MTBE doses. Particularly interesting is the evolution of the complex band at 2828 cm^{-1} (assignment in Table 2) upon pressure decreasing, in that a component at 2843 cm^{-1} is more clearly visible at very low MTBE doses (Fig. 9B, curves g-s), and this suggests that the molecule experiences two different environments. As already noticed at low pressure MTBE is bound to silanols, whereas at higher pressure molecules are adsorbed on to the zeolite framework by van der Waals forces. It is thus clear that the redistribution of the electronic charge of the MTBE oxygen atom, which occurs when the molecule is H-bonded to silanol groups, significantly influences the frequency of CH_3 stretching vibrations of the methoxyl radical. This vibrational mode can be therefore used to monitor the state/phase of the molecules adsorbed on the zeolite.

The structures of two MTBE-zeolite complexes were optimized at the DFT level, using the model of the HSZ-Y cage described above and illustrated in Figure 3, a. As said above, in the present model a defect was introduced in the cage wall, forming an isolated silanol group available for binding the guest molecule. The

two model complexes, shown in Figures 3 b and c, comprise one and three MTBE molecules, respectively, to reproduce the adsorption regimes at low and high pressure described above.

With a single MTBE the optimization leads to a H-bond between the cage silanol and the guest molecule, with an O-O distance of 2.69 Å, slightly smaller than the distance (2.71 Å) in the complex with the cluster shown in Figure 2, which accounts for the experimental shifts very well: then, the silanol inside the model cage is somehow too polarized with respect to the free group in the small model. This feature can be due to the large number of mesopores in this kind of zeolite, so that the silanol groups are better described by silica clusters than by the tight cage model.

When two other guest molecules are added, they adjust to optimize the van der Waals interactions with the cage walls and with the first MTBE: the geometry relaxation shows that three MTBE molecules can easily accommodate inside the cage, causing a small reduction of the ether-silanol H-bond length. This effect may account for the increase of the relative intensity of the band at 3240 cm^{-1} when MTBE pressure is increased to 30 mbar (Fig. 8 curve c).

Conclusions

The effect of the silanol groups contained in a high silica zeolite Y (HSZ-Y, SiO_2/Al_2O_3 = 200) on the adsorption of methyl *tertiary* butyl ether (MTBE) was evaluated. As defined by pore size analysis, the dealumination process generates a number of structural defects in zeolite Y, so that a relevant pore fraction merges to the diameter of 22 Å (11 Å being the pore diameter of standard zeolite Y). The thermogravimetric analysis shows that the amount of point defects (i.e. silanol groups) is attested on average at three silanol groups per zeolite α cage.

The silanol types occurring in the dehydrated zeolite Y (outgassed at room temperature) was determined by infrared spectroscopy. The frequencies associated to isolated and H-bond acceptor silanol groups were assigned in the spectrum at 3746 and 3530 cm^{-1}, respectively, while H-bond donor silanols stretching was masked by other modes. The interpretation of the IR spectra was supported by DFT calculations on different models of silanols and silanol-MTBE complexes.

The contribution of the different groups to the adsorption was better clarified by outgassing the zeolite at 700°C, thus leaving only isolated silanols, both on external and internal surfaces. The adsorption isotherm of the outgassed sample and the IR spectra after the MTBE loading show that, at pressures below 1.25 mbar, MTBE is adsorbed through H-bonding to silanols, the maximum loading in this stage being 1.3 molecules per zeolite cage. At higher pressures a second regime is observed in the isotherm, corresponding to adsorption driven by hydrophobic interactions, with an additional loading of 1.3 molecules per cage. Two models of MTBE confined in the cage (comprising one and three ether molecules, respectively) were optimized at the DFT level, showing that the first molecule binds to the internal silanol, while the other molecules accommodate in the cage with a little perturbation of the MTBE-silanol complex.

At low MTBE dosage (below 1.25 mbar), the downward shifts of stretching modes for isolated silanols are consistent with medium-weak H-bonding with MTBE oxygen, being 516 cm^{-1} and 358 cm^{-1} for external and internal silanols, respectively. Due to the cage confinement effects, the MTBE appears to interact more strongly with isolated silanols on the internal than on external surface, though the latter provide stronger H-bonding to the molecule according to IR analysis. At higher MTBE dosage (1.25 ÷ 30 mbar), no silanol groups remain available and the adsorption occurs at the siloxane network of the zeolite. Interestingly, the band of the methyl symmetric stretching in CH_3O- is very sensitive to the MTBE-zeolite interactions, either H-bonding or hydrophobic: in the former case it is found at ca. 2843 cm^{-1}, in the latter it is downshifted of 15 cm^{-1} to 2828 cm^{-1}. On the other hand, H-bond acceptor silanol groups do not contribute to the MTBE-zeolite interaction significantly, as shown by the comparison of the adsorption isotherms for samples outgassed at room temperature and at 400°C.

Due to the large number of mesopores inside this kind of zeolite, we found that the internal silanols are better modeled with silica clusters than with defects in single zeolite cages.

In conclusion, under the experimental conditions used in this study, the silanol fraction of the high silica zeolite Y is favored with respect to the siloxane network in the adsorption of MTBE, with the retention strength in the order: internal silanol > external silanol > siloxane fraction. In the light of these findings, beside the silica content also the point defects of zeolites should be considered for the adsorption process:

this conclusion also applies to aqueous solutions, which are the actual working conditions of these materials, for MTBE is known to be able to displace water from zeolite isolated silanols.

Acknowledgment

Research co-funded by Research Center for Non-Conventional Energy, Istituto ENI Donegani – Environmental Technologies (Novara, Italy). J. Vitillo (NIS), M. Mercer and C. Cook (Mercer Instruments) are gratefully acknowledged for constant help and support for gravimetric measurements.

References

[1] Squillace, P. J.; Pankow, J. F.; Kortes, N. E.; Zogorski, J. S. *Environmental Behavior and Fate of Methyl tert-Butyl Ether (MTBE)*; U.S. Department of the Interior, U.S. Geological Survey, National Water Quality Assessment Program (NAWQA), USGS Series Fact Sheet, USGS Library Call Number (200)F327 No. 96-203, 1996.

[2] Office of Environmental Health Hazard Assessment. *Public Health Goal for Methyl Tertiary Butyl Ether (MTBE) in Drinking Water*; OEHHA, California EPA, 1999.

[3] Environmental Protection Agency. *2002 Edition of the Drinking and Health Advisories*; Washington, DC, U.S.A., 2002.

[4] Erdem-Şenatalar, A.; Bergendahl, J. A.; Giaya, A.; Thompson, R. W. *Environ. Eng. Sci*. **2004**, *21*, 722.

[5] Knappe, D. R. U.; Campos, A. A. R. *Water Sci. Technol.: Water Supply* **2005**, *5*, 83.

[6] Anderson, M. A. *Environ. Sci. Technol.* **2000**, *34*, 725.

[7] Shiguang, L.; Tuan, V. A.; Noble, R. D.; Falconer, J. L. *Environ. Sci. Technol.* **2003**, *37*, 4007.

[8] A. O. Yazaydin, R. W. Thompson. *J. Phys. Chem. B* **2006,** *110*, 14458-14462.

[9] A. Rossner. D. R. U. Knappe. *Water Res*. **2008**, *42*, 2287-2299.

[10] T. Armaroli, M. Trombetta, A. G. Alejandre, J. R. Solis, G. Busca. *Phys. Chem. Chem. Phys*. **2000**, *2*, 3341-3348.

[11] M. A. Anderson. *Environ. Sci. Technol*. **2000**, *34*, 725-727.

[12] A. Zecchina, S. Bordiga, G. Spoto, L. Marchese, G. Petrid, G. Leofanti, M. Padovan. *J. Phys. Chem.* **1992**, *96*, 4991-4997.

[13] S. Tosoni, B. Civalleri, F. Pascale, P. Ugliengo. *J. Phys.: Conference Series* **2008,** *1,* 1-8.

[14] R. Ahlrichs, M. Bar, M. Haser, H. Horn, C. Kolmen, *Chem. Phys. Lett.* **1989**, *162*, 165.

[15] M. Arnim, R. Ahlrichs, *J. Chem. Phys*. **1999**, *111*, 9183.

[16] A. D. Becke, *Phys. Rev. B*, **1988**, *38*, 3098.

[17] C. Lee, W. Yang, R. G. Parr, *Phys. Rev.* **1988**, *37*, 785.

[18] A. D. Becke, *J. Chem. Phys.* **1993**, *98*, 1372.

[19] P. C. Hariharan, P. C., J. A. Pople, *Theor. Chim. Acta* **1973**, *28*, 213.

[20] T. H. Dunning, *J. Chem. Phys.* **1989**, *90*, 1007.

[21] P. J. Hay, W. R. Wadt, *J. Chem. Phys*., **1985**, *82*, 299.

[22] I. Braschi, G. Gatti, G. Paul, C. E. Gessa, M. Cossi, L. Marchese. *Langmuir* **2010**, *26*, 9524-9532.

[23] I. Braschi, S. Blasioli, L. Gigli, C. E. Gessa, A. Alberti, A. Martucci. *J. Hazard. Mat.* **2010**, *178*, 218-225.

[24] R. Szostak, Secondary synthesis methods, In: Introduction to zeolite science and practice. 2nd completely revised and expanded edition.

[25] H. Van Bekkum, E.M. Flanigen, P.A. Jacobs, J.C. Jansen (Eds) *Stud. Surf. Sci. Catal.* **2001**, *137*, 261-272.

[26] T. Kawai, K. Tsutsumi. *Adsorption* **1998**, *4*, 225-231.

[27] J.M.R. Gallo, C. Bisio, G. Gatti, L. Marchese, H.O. Pastore. *Langmuir* **2010,** 26, 5791-5800.

[28] Z. Li, S. Singh, *J. Phys. Chem. A*, **2008**, *112*, 8593-8599

[29] F. Carniato, G. Paul, C. Bisio, S. Caldarelli, L. Marchese, *RSCAdvances*, DOI: 10.1039/C1RA00460C

Table 1. Main textural properties of high silica zeolite Y (HSZ-Y). Data for non dealuminated standard zeolite Y (SZ-Y) are reported for comparison.

Sample	SSA_{BET}[a] ($m^2\ g^{-1}$)	SSA_{microp}[b] ($m^2\ g^{-1}$)	V_P[c] ($cm^3\ g^{-1}$)	V_{microp}[d] (≤20 Å) ($cm^3\ g^{-1}$)	V_{mesop}[d] (20÷40 Å) ($cm^3\ g^{-1}$)
HSZ-Y	902	437	0.52	0.32	0.16
SZ-Y	769	543	0.65	0.47	-

[a] Brunauer–Emmet–Teller (BET) specific surface area (SSA)

[b] Micropore surface area by t-plot method

[c] Total pore volume by NLDFT method

[d] Volume calculated by NLDFT method

Table 2. Infrared wavenumber (cm^{-1}) for methyl *tertiary* butyl ether (MTBE) computed *in vacuo* and experimentally obtained in gas and in CCl_4 solution and adsorbed into high silica zeolite Y (HSZ-Y) dehydrated at room temperature.

Vibrational mode	**Computed**	**MTBE in gas phase**	**MTBE in CCl_4**	**MTBE adsorbed into HSZ-Y (1.25 mbar)**	**MTBE adsorbed into HSZ-Y (30 mbar)**
ν_{asym} *t*-butyl CH_3	3121	2985	2974	2979	2976
ν_{asym} methoxyl CH_3	3072	2946	2939	2945	2942
ν_{sym} *t*-butyl CH_3	3037	2917	2906	2917	2914
ν_{sym} methoxyl CH_3	3011	2835	2827	2830	2828
$def_{out\text{-}of\text{-}phase}$ methoxyl & *t*-butyl CH_3	1550	1470	1469	1473	1473
$def_{out\text{-}of\text{-}phase}$ methoxyl & *t*-butyl CH_3	1520	1458	n.a.	n.a.	n.a.
$def_{in\text{-}phase}$ *t*-butyl CH_3	1450	1386	1386	1390	1388
$def_{in\text{-}phase}$ *t*-butyl CH_3	1420	1364	1364	1369	1366
δ C-O-C + $def_{out\text{-}of\text{-}phase}$ methoxyl & butyl CH_3	1300	-	1261	n.a.	n.a.
ν_{asym} *t*-butyl C-C	1264	-	1232	n.a.	n.a.
ν_{asym} *t*-butyl C-O	1224	1209	1204	n.a.	n.a.
ν_{asym} methoxyl C-O	1091	1096	1085	n.a.	n.a.

n.a.: not available because overlapped with zeolite vibrational modes

Figure Captions

Figure 1. Schematic representation of silanol groups considered in this work: (1) isolated; (2) H-bond donor; (3) H-bond acceptor.

Figure 2. (a) $Si_{13}O_{13}H_{39}(OH)$ cluster used to model an isolated silanol; (b) $Si_{13}O_{13}H_{38}(OH)_2$ cluster used to model a couple of H-bonded silanols; (c) adduct of MTBE to isolated silanol; (d) adduct of MTBE to H-bond acceptor silanol. Stretching wavenumber for silanol groups are reported.

Figure 3. (a) Model of zeolite Y cage with a single defect (i.e. silanol); (b) Model of the MTBE in zeolite cage: a single ether H-bonded to the defect silanol; (c) Model of the MTBE in zeolite cage: three ether molecules inside the cage.

Figure 4. Pore diameter distribution of high silica zeolite Y (HSZ-Y) by nitrogen adsorption isotherm (see inset) at -196°C using a cylindrical pore NLDFT method in the desorption branch. Pore size distribution of standard zeolite Y (SZ-Y) is reported as a comparison.

Figure 5. High silica zeolite Y treated in vacuum at increasing temperature: A) sample in air (a), after ougassing at room temperature (b), and at 100, 250, 400, 550, 700°C (c-g). All spectra were recorded at beam temperature; A inset) Zeolite Y before (curve a) and after (curve b) outgassing at room temperature (bending of water at 1633 cm^{-1}); B) enlargement of spectral region of external and internal silanol groups at 3746 and 3738 cm^{-1}, respectively).

Figure 5. High silica zeolite Y treated in vacuum at increasing temperature: A) Sample in air (a), and after ougassing at room temperature, 100, 250, 400, 550, 700°C (b-g). All spectra were recorded at beam temperature; A inset) Zeolite before and after outgassing at room temperature (bending of water at 1633 cm^{-1}); B) Enlargement of spectral region of external and internal silanol groups at 3746 and 3738 cm^{-1}, respectively.

Figure 6. MTBE gravimetric adsorption (–o–) and desorption (–•–) isotherms measured at 35°C on high silica zeolite Y. The MTBE uptake at 1.25, 10, and 30 mbar of MTBE pressure was 8.1, 15.1, and 16.4% zeolite dry weight corresponding to 1.3, 2.4, and 2.6 MTBE molecules per zeolite cage, respectively.

Figure 7. Computed (a) and experimental infrared spectra of MTBE in gas phase (b) and in carbon tetrachloride solution (c). * Bands due to carbon tetrachloride.

Figure 8. Infrared spectra of high silica zeolite Y outgassed at room temperature (a) and exposed to 1.25 mbar (b) and 80 mbar (c) of MTBE.

Figure 9. Differential infrared spectra of increasing doses of MTBE adsorbed on high silica zeolite Y outgassed at 700°C; spectra upon exposure of zeolite sample at the following MTBE pressure: a) 2.5, b) 1.9, c) 1.6, d) 1.2, e) 0.9, f) 0.7, g) 0.5, h) 0.35, i) 0.26, l) 0.19, m) 0.13, n) 0.08, o) 0.045, p) 0.028, q) $3 \cdot 10^{-3}$ mbar. The spectrum of the bare sample was used as reference and subtracted from all spectra obtained after exposure of MTBE vapour. In the insets, enlarged view of the spectral region between 3800-3650 and 2875-2775 cm^{-1} is reported.

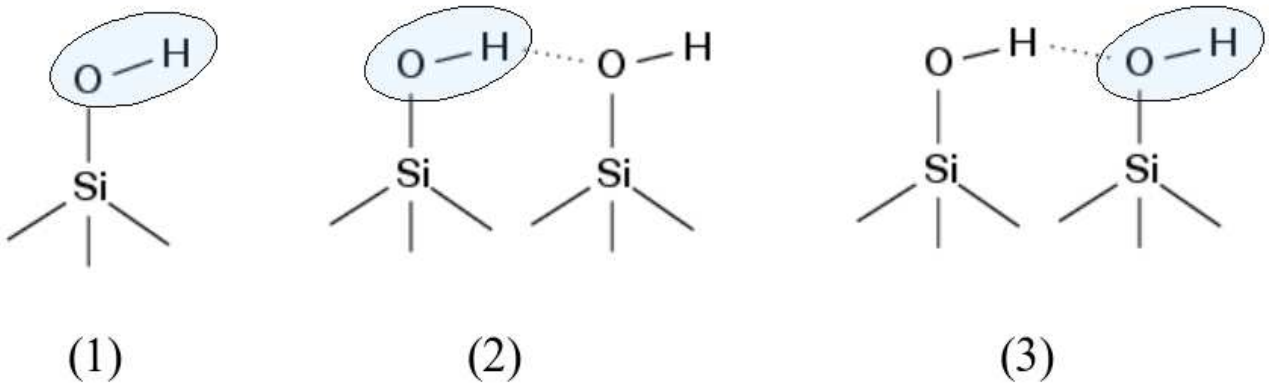

Figure 1. Schematic representation of silanol groups considered in this work: (1) isolated; (2) H-bond donor; (3) H-bond acceptor.

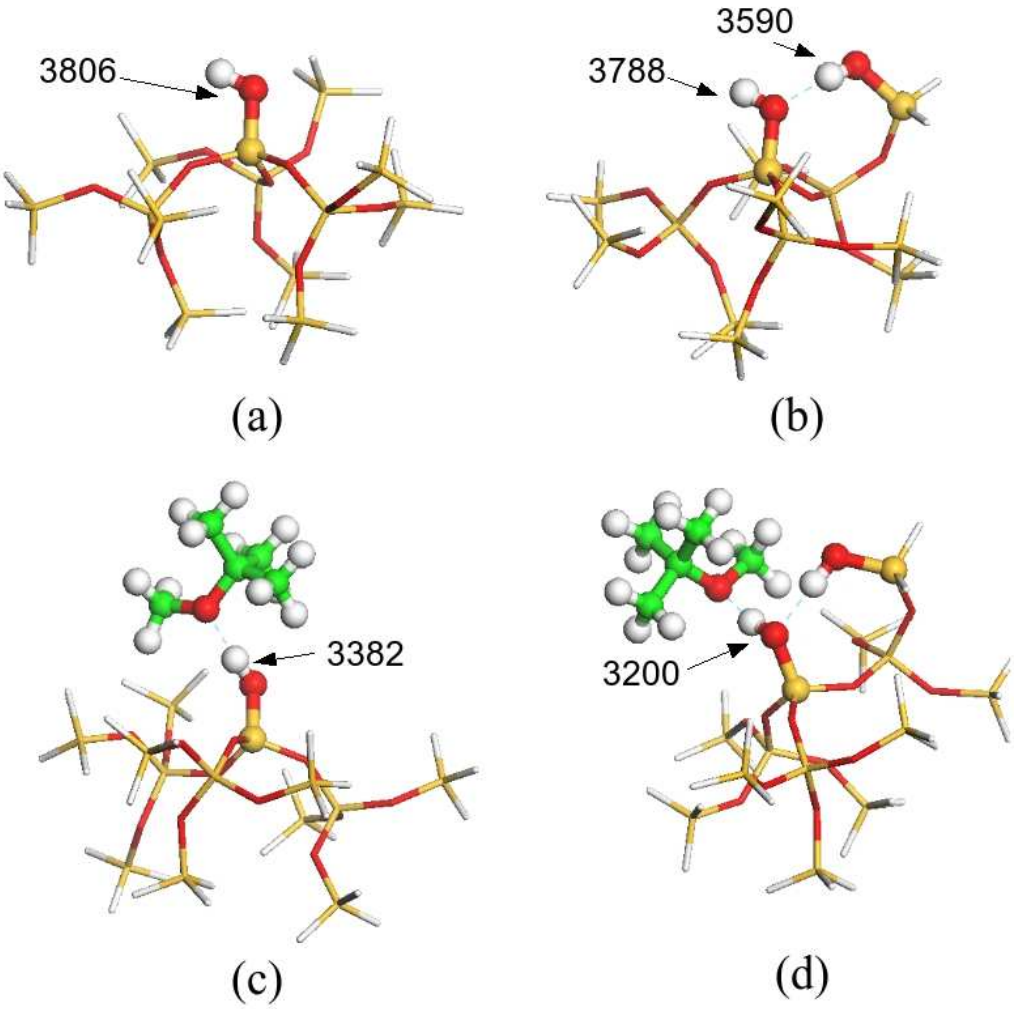

Figure 2. (a) $Si_{13}O_{12}H_{27}(OH)$ cluster used to model an isolated silanol; (b) $Si_{13}O_{11}H_{26}(OH)_2$ cluster used to model a couple of H-bonded silanols; (c) adduct of MTBE to isolated silanol; (d) adduct of MTBE to H-bond acceptor silanol. Stretching wavenumber for silanol groups are reported.

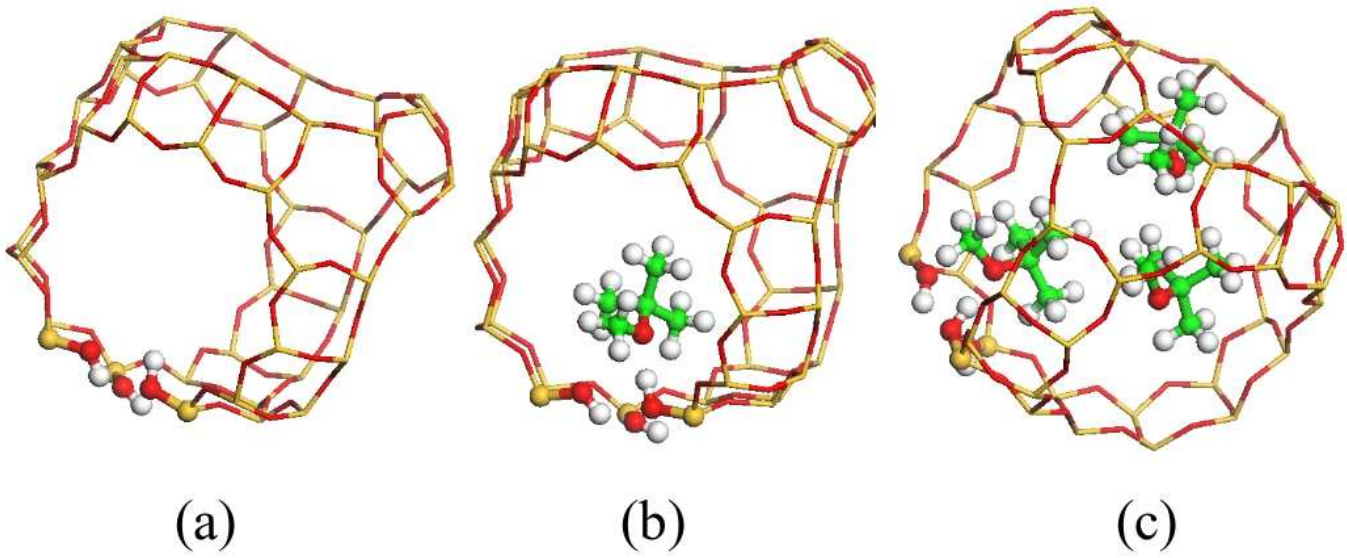

Figure 3. (a) Model of zeolite Y cage with a single defect (i.e. silanol); (b) Model of the MTBE in zeolite cage: a single ether H-bonded to the defect silanol; (c) Model of the MTBE in zeolite cage: three ether molecules inside the cage.

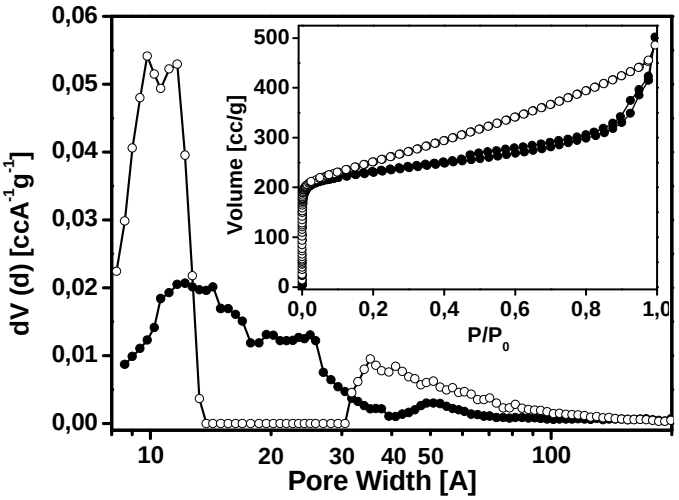

Figure 4. Pore diameter distribution of high silica zeolite Y (HSZ-Y) by nitrogen adsorption isotherm (see inset) at -196°C using a cylindrical pore NLDFT method in the desorption branch. Pore size distribution of standard zeolite Y (SZ-Y) is reported as a comparison.

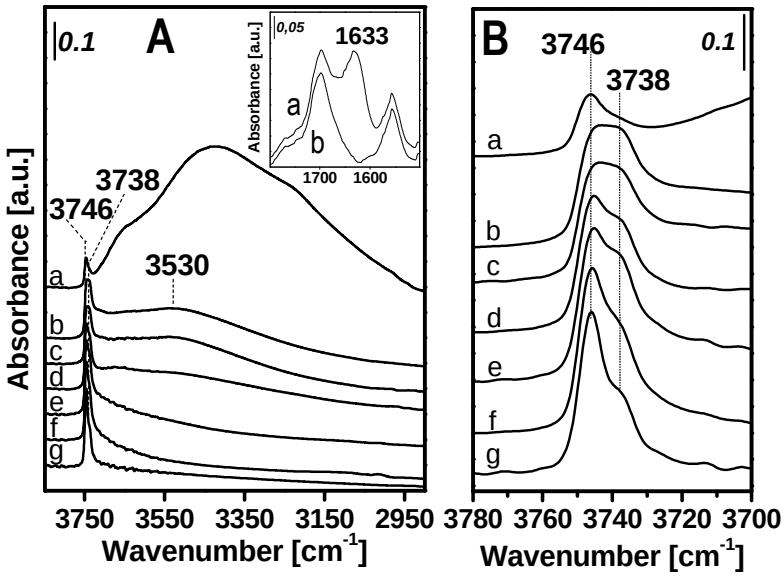

Figure 5. High silica zeolite Y treated in vacuum at increasing temperature: A) sample in air (a), after ougassing at room temperature (b), and at 100, 250, 400, 550, 700°C (c-g). All spectra were recorded at beam temperature; A inset) Zeolite Y before (curve a) and after (curve b) outgassing at room temperature (bending of water at 1633 cm^{-1}); B) enlargement of spectral region of external and internal silanol groups at 3746 and 3738 cm^{-1}, respectively).

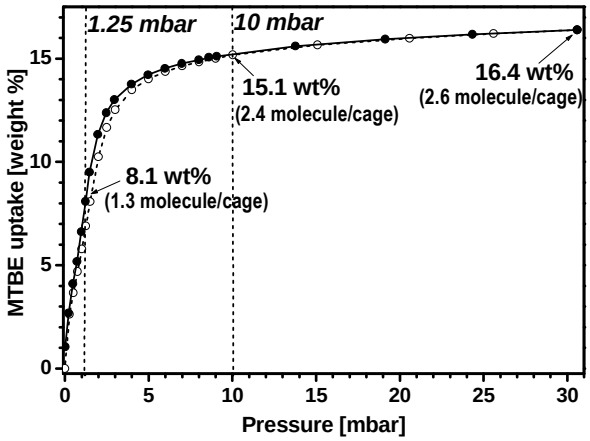

Figure 6. MTBE gravimetric adsorption (–o–) and desorption (–•–) isotherms measured at 35°C on high silica zeolite Y. The MTBE uptake at 1.25, 10, and 30 mbar of MTBE pressure was 8.1, 15.1, and 16.4% zeolite dry weight corresponding to 1.3, 2.4, and 2.6 MTBE molecules per zeolite cage, respectively.

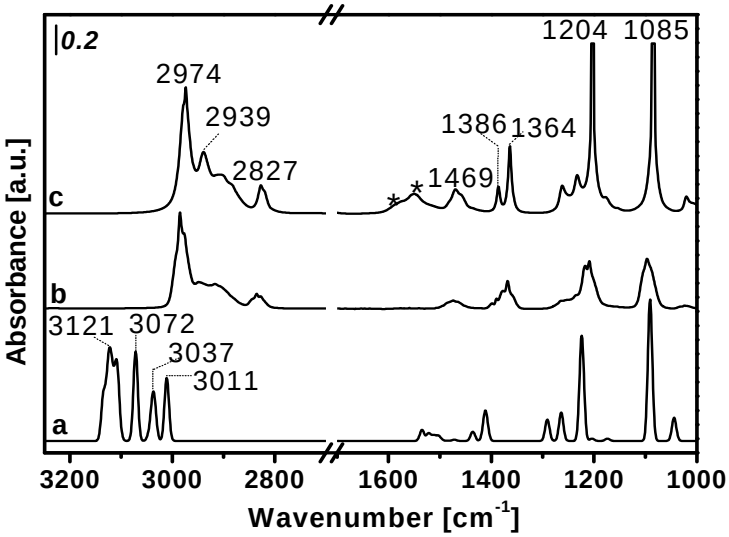

Figure 7. Computed (a) and experimental infrared spectra of MTBE in gas phase (b) and in carbon tetrachloride solution (c). * Bands due to carbon tetrachloride.

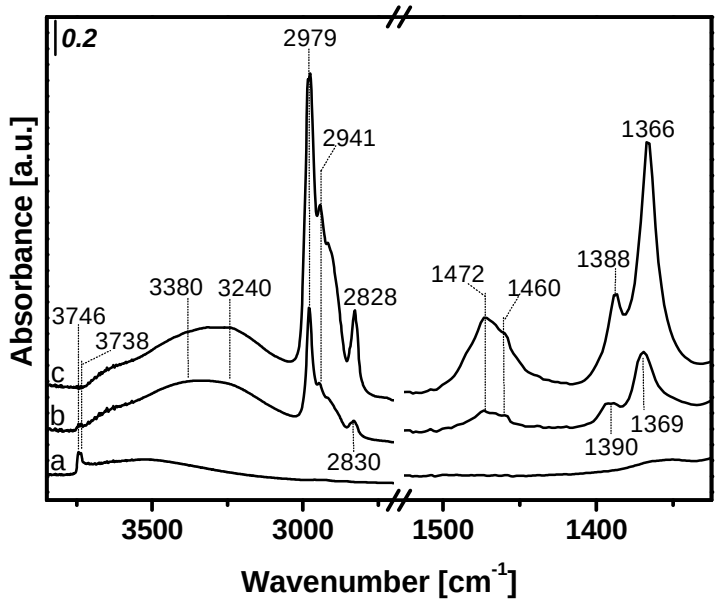

Infrared spectra of high silica zeolite Y outgassed at room temperature (a) and exposed to 1.25 mbar (b) and 30 mbar (c) of MTBE.

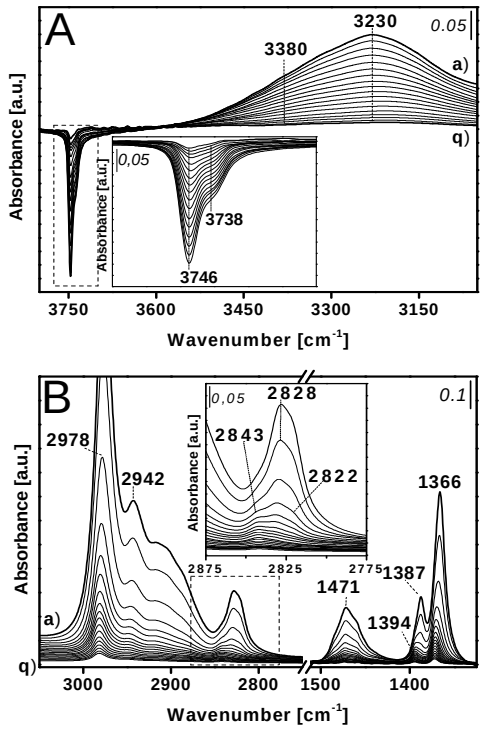

Figure 9. Differential infrared spectra of increasing doses of MTBE adsorbed on high silica zeolite Y outgassed at 700°C; spectra upon exposure of zeolite sample at the following MTBE pressure: a) 2.5, b) 1.9, c) 1.6, d) 1.2, e) 0.9, f) 0.7, g) 0.5, h) 0.35, i) 0.26, l) 0.19, m) 0.13, n) 0.08, o) 0.045, p) 0.028, q) $3 \cdot 10^{-3}$ mbar. The spectrum of the bare sample was used as reference and subtracted from all spectra obtained after exposure of MTBE vapour. In the insets, enlarged view of the spectral region between 3800-3650 and 2875-2775 cm^{-1} is reported.